Topological Blount's theorem of odd-parity superconductors

Shingo Kobayashi,[1] Ken Shiozaki,[2] Yukio Tanaka,[1] and Masatoshi Sato[1]
[1]*Department of Applied Physics, Nagoya University, Nagoya 464-8603, Japan*
[2]*Department of Physics, Kyoto University, Kyoto 606-8502, Japan*
(Received 7 April 2014; revised manuscript received 23 June 2014; published 23 July 2014)

Blount's theorem prohibits the existence of line nodes for odd-parity superconductors (SCs) in the presence of spin-orbit coupling (SOC). We studied the topological stability conditions of line nodes under inversion symmetry by generalizing the original statement and establishing a relation to surface zero-energy states. The topological instability of line nodes in odd-parity SCs implies the disappearance of corresponding flat zero-energy surface dispersions due to surface Rashba SOC, which provides an experimental means to distinguish line nodes in odd-parity SCs from those in other SCs.

DOI: 10.1103/PhysRevB.90.024516 PACS number(s): 74.20.−z, 73.20.−r, 74.25.−q, 74.70.Tx

I. INTRODUCTION

Nontrivial nodal structures are an important feature in unconventional superconductors (SCs). The existence of nodes provides a clue into the symmetry of Cooper pairings and is influential in power law behaviors of temperature dependencies such as the specific heat and NMR relaxation rates [1,2]. In the 1980s, heavy fermion materials attracted much attention as a candidate of unconventional SCs. By taking into account strong spin-orbital coupling (SOC) in heavy fermion materials, Cooper pairs were classified based on the group theory where symmetry operation on the crystal lattices is followed by the spin. Using this, Blount proved the impossibility of line nodes in odd-parity SCs [3]. By assuming a time-reversal-invariant single-band spin-triplet Cooper pair, he showed that a large region of zero gap is "vanishingly improbable" in the presence of SOC. This statement is now known as Blount's theorem. Conversely, real candidate materials of heavy fermion odd-parity SCs such as UPt_3 [4] have often suggested the existence of line nodes. This is because the actual influence of SOC in bulk Cooper pairs is strongly suppressed by the Fermi energy [5]. Indeed, as these materials always do, if the normal state has inversion symmetry (IS) and time-reversal symmetry (TRS), the SOC retains the spin degeneracy of the Fermi surface, so its influence is merely a small deformation of the Fermi surface or a perturbative contribution to the pairing interaction. As such, the implication of Blount's theorem had been uncertain.

Whereas Blount used group theoretical arguments to prove his theorem, there are other arguments for the stability of line nodes [6,7] in which the nodal structures are classified by topological invariants [8–10]. Without assuming a large SOC, this method enables us to treat both the symmetric and accidental nodes in a unified way, as well as include the influence of normal states and multiband structures. In particular, the topological method has an advantage in that it may connect topological structures of bulk nodes to surface flatbands via the bulk-boundary correspondence [11–18] [see Fig. 1(b)]. In contrast to bulk Cooper pairs, the surface states may be strongly affected by SOC because the boundary breaks IS, inducing the surface Rashba SOC. Such an antisymmetric SOC is directly coupled to the surface states as well as the surface Cooper pair, lifting the spin degeneracy. Therefore the topological classification has the potential to extend the original Blount's theorem and provide novel implications for experimental measurement.

In this paper, we generalize Blount's theorem in terms of K theory [19,20] and extend it to surface flatbands. The purpose of this paper is to prove the following statements: (i) A line node in odd-parity SCs is topologically unstable with or without TRS in the absence of additional symmetry. (ii) An additional symmetry such as mirror symmetry or spin-rotation symmetry (SRS) may stabilize the bulk line node in odd-parity SCs, but the corresponding surface flatband is fragile and disappears due to the surface Rashba SOC. Hence it is possible to distinguish odd-parity Cooper pairs from even-parity or noncentrosymmetric ones by the behavior of the flatband.

II. FORMULATION

We start with the Bogoliubov–de Gennes (BdG) Hamiltonian:

$$H = \frac{1}{2}\sum_{\boldsymbol{k},\alpha,\alpha'} (c^{\dagger}_{\boldsymbol{k}\alpha}, c_{-\boldsymbol{k}\alpha}) H(\boldsymbol{k}) \begin{pmatrix} c_{\boldsymbol{k}\alpha'} \\ c^{\dagger}_{-\boldsymbol{k}\alpha'} \end{pmatrix}, \tag{1}$$

where $H(\boldsymbol{k})$ is given by

$$H(\boldsymbol{k}) = \begin{pmatrix} \epsilon(\boldsymbol{k})_{\alpha\alpha'} & \Delta(\boldsymbol{k})_{\alpha\alpha'} \\ \Delta(\boldsymbol{k})^{\dagger}_{\alpha\alpha'} & -\epsilon(-\boldsymbol{k})^{T}_{\alpha\alpha'} \end{pmatrix}. \tag{2}$$

$c^{\dagger}_{\boldsymbol{k}\alpha}$ ($c_{\boldsymbol{k}\alpha'}$) represents the creation (annihilation) operator of an electron with momentum $\boldsymbol{k}$. The suffix α represents other degrees of freedom such as spin, orbital, and sublattice indices. $\epsilon(\boldsymbol{k})_{\alpha\alpha'}$ and $\Delta(\boldsymbol{k})_{\alpha\alpha'}$ are the Hamiltonian in the normal state and gap function, respectively. For the case of a single-band spin-triplet Cooper pair, the gap function is given by $\Delta(\boldsymbol{k}) = i\boldsymbol{d}(\boldsymbol{k})\cdot\boldsymbol{\sigma}\sigma_y$, where $\boldsymbol{\sigma}$ is the Pauli matrix, and the $\boldsymbol{d}$ vector satisfies $\boldsymbol{d}(-\boldsymbol{k}) = -\boldsymbol{d}(\boldsymbol{k})$ [$d_i \in \mathbb{R}$ ($i = x,y,z$) if TRS exists]. The BdG Hamiltonian naturally has particle-hole symmetry (PHS) such that

$$CH(\boldsymbol{k})C^{\dagger} = -H(-\boldsymbol{k}), \quad C^2 = 1. \tag{3}$$

Also, TRS is defined by

$$TH(\boldsymbol{k})T^{\dagger} = H(-\boldsymbol{k}), \quad T^2 = -1, \tag{4}$$

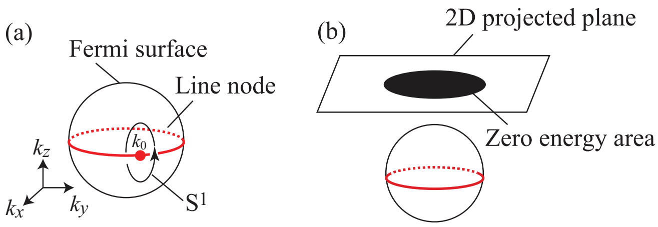

FIG. 1. (Color online) (a) A line node of the p_z-wave SC is wrapped by S^1. $\boldsymbol{k}_0$ indicates the position of the node. (b) The projection of the line node on the two-dimensional plane with a fixed k_z. The zero-energy state appears at the black color area if the open boundary condition for the z axis is imposed.

where C and T are antiunitary. In addition, we assume IS such that

$$P\epsilon(\boldsymbol{k})P^\dagger = \epsilon(-\boldsymbol{k}), \quad P\Delta(\boldsymbol{k})P^T = \eta_C^P\Delta(-\boldsymbol{k}), \tag{5}$$

where P acts on the creation (annihilation) operator as $c^\dagger_{\boldsymbol{k}\alpha} \to P^*_{\alpha\alpha'}c^\dagger_{-\boldsymbol{k}\alpha'}$ ($c_{\boldsymbol{k}\alpha} \to P_{\alpha\alpha'}c_{-\boldsymbol{k}\alpha'}$) and satisfies $P^2 = 1$. The factor η_C^P specifies either even parity ($\eta_C^P = 1$) or odd parity ($\eta_C^P = -1$) of the gap function. In the Nambu representation, we denote P as $\tilde{P} = \mathrm{diag}(P,\eta_C^P P^*)$ [21]. The parity of the gap function determines the commutation or anticommutation relation between C and $\tilde{P}$: $[C,\tilde{P}] = 0$ ($\{C,\tilde{P}\} = 0$) for even-parity (odd-parity) pairings. Also, note that $[T,\tilde{P}] = 0$ because P does not act on the spin space.

III. STABILITY OF NODE AND SYMMETRY

A node of SCs is a set of $\boldsymbol{k}$ satisfying $\det H(\boldsymbol{k}) = 0$. In d dimensions, the node with codimension $p+1$ defines a $(d-p-1)$-dimensional submanifold Σ. For example, a line node in three dimensions has a codimension of 2, and it defines a one-dimensional manifold along the node. If we consider a symmetry-preserving small perturbation of H, the node either slightly shifts its position or completely vanishes due to the emergence of a gap. The former implies that the node is topologically stable because it cannot vanish by small perturbations.

To precisely define the topological stability of the node, we consider a small p-dimensional sphere S^p wrapping around the node at $\boldsymbol{k}_0 \in \Sigma$ (see Fig. 1). Then the Hamiltonian defines a map, $\boldsymbol{k} \in S^p \mapsto H(\boldsymbol{k}) \in \mathcal{Q}$, from S^p to a classifying space $\mathcal{Q}$ of matrices subject to symmetries defined in Eqs. (3), (4), and (5). A homotopy equivalence class of the map is given by the homotopy group $\pi_p(\mathcal{Q})$. If the node has a nontrivial topological number of $\pi_p(\mathcal{Q})$, we cannot eliminate the node because the Hamiltonian with the node does not continuously connect to that with a gap.

Here we may assume without loss of generality that the BdG Hamiltonian near a node $\boldsymbol{k}_0$ is given by

$$H_{\boldsymbol{k}_0}(\boldsymbol{p}) := H(\boldsymbol{k}_0+\boldsymbol{p}) \simeq \sum_{i=1}^{p+1} v_i p_i \gamma_i, \tag{6}$$

where v_i is an expansion coefficient, $|\boldsymbol{p}| \ll 1$, and the γ matrices $(\gamma_1,\ldots,\gamma_{p+1})$ satisfy the Clifford algebra, $\{\gamma_i,\gamma_j\} = 2\delta_{ij}$. $H_{\boldsymbol{k}_0}(\boldsymbol{p})$ describes the dispersion of $\boldsymbol{p}$ near the node, which is determined by $\epsilon(\boldsymbol{k})$ and $\Delta(\boldsymbol{k})$ of the underlying BdG Hamiltonian [22]. Imposed symmetry of $H_{\boldsymbol{k}_0}(\boldsymbol{p})$ depends on whether the node $\boldsymbol{k}_0$ is located on a symmetric point satisfying $\boldsymbol{k}_0 = -\boldsymbol{k}_0 + \boldsymbol{G}$, where $\boldsymbol{G}$ is a reciprocal lattice vector. If $\boldsymbol{k}_0 = -\boldsymbol{k}_0 + \boldsymbol{G}$, the position of the node remains unchanged under C, T, $\tilde{P}$. Thus the symmetry operation on $H_{\boldsymbol{k}_0}$ is identical to the underlying BdG Hamiltonian (2). Conversely, if $\boldsymbol{k}_0 \neq -\boldsymbol{k}_0 + \boldsymbol{G}$, the position of the node changes into its inverse under C, T, and $\tilde{P}$. Thus these operations are not the symmetry of $H_{\boldsymbol{k}_0}$. Appropriate symmetries are given by the combination of them such that

$$(C\tilde{P})H_{\boldsymbol{k}_0}(\boldsymbol{p})(C\tilde{P})^\dagger = -H_{\boldsymbol{k}_0}(\boldsymbol{p}), \tag{7}$$

$$(T\tilde{P})H_{\boldsymbol{k}_0}(\boldsymbol{p})(T\tilde{P})^\dagger = H_{\boldsymbol{k}_0}(\boldsymbol{p}). \tag{8}$$

Topological stability of nodes at $\boldsymbol{k}_0 = -\boldsymbol{k}_0 + \boldsymbol{G}$ have been discussed in Refs. [10,23], in which PHS and TRS were taken into account separately. In addition, the topological stability of nodes are directly connected to the Altland-Zirnbauer (AZ) symmetry classes [24,25] of the bulk electronic state [18,26]. However, nearly all the nodes in SCs appear on the Fermi surface and obey $\boldsymbol{k}_0 \neq -\boldsymbol{k}_0 + \boldsymbol{G}$. Thus it is valuable to discuss the node stabilities with the symmetries described by Eqs. (7) and (8) as a physically realistic situation. Hereafter, we use the combined symmetries to classify stable nodes.

IV. PHS, TRS, AND LINE NODE

To identify the classifying space of $H_{\boldsymbol{k}_0}$, we employ the Clifford algebra extension method [27–31], which enables us to reduce the problem to the description of possible Dirac mass terms. However, $H_{\boldsymbol{k}_0}$ has no mass term. Nevertheless, we can apply this method to it by regarding one of the γ matrices as the mass term, e.g., γ_{p+1}, because the base space S^p is compacted. According to Eqs. (7) and (8), we impose only $C\tilde{P}$ on SCs with IS, and both $C\tilde{P}$ and $T\tilde{P}$ on SCs with IS and TRS. Herein, we denote the former (latter) systems as a P+D (P+DIII) class, the classifying space of which depends on either the even parity ($[C,\tilde{P}] = 0$) or odd parity ($\{C,\tilde{P}\} = 0$).

By systematically searching for the possible mass terms, we achieve the classifying spaces and topological numbers for each class and each codimension, as listed in Table I, in which we add the topological classification without IS (D and DIII classes) for comparison. These classifying spaces are calculated by the Clifford algebra extension method, which is shown in Appendix 2. We label the classifying spaces as C_i ($i = 0,1$) and R_j ($j = 0,1,2,\ldots,7$) according to the conventional way [27–31]. Note that the higher-dimensional homotopy groups in the present case are calculated by $\pi_p(C_i) = \pi_0(C_{i+p})$ and $\pi_p(R_j) = \pi_0(R_{j+p})$. In particular, when $p = 1$, Table I shows the line node stability. Hence topologically stable line nodes can exist for the DIII and P+DIII classes with even parity [6,7,14]. In fact, this accounts for the stability of line nodes in noncentrosymmetric SCs such as $CePt_3Si$ [32,33] and high-T_c materials [34–36]. Conversely, Table I implies that line nodes in odd-parity SCs are topologically unstable with or without TRS. The latter statement is one of the main results of the present article.

TABLE I. Node classifications, which occur at $\boldsymbol{k}_0 \neq -\boldsymbol{k}_0 + \boldsymbol{G}$, in the system with C, T, and $\tilde{P}$. The first, second, third, and fourth columns show the symmetry classes, symmetry constraint for each class, parity of gap functions, and classifying space $\mathcal{Q}$, respectively. The remaining columns show the topological classification for $p = 0$, 1, and 2. In 3D, each codimension represents a surface node, line node, and point node, respectively.

Class	Symmetry	Parity	$\mathcal{Q}$	$p=0$	$p=1$	$p=2$
D	$\{1\}$	N/A	C_0	$\mathbb{Z}$	0	$\mathbb{Z}$
DIII	$\{CT\}$	N/A	C_1	0	$\mathbb{Z}$	0
P+D	$\{C\tilde{P}\}$	Even	R_2	$\mathbb{Z}_2$	0	$2\mathbb{Z}$
		Odd	R_6	0	0	$\mathbb{Z}$
P+DIII	$\{C\tilde{P},T\tilde{P}\}$	Even	R_3	0	$2\mathbb{Z}$	0
		Odd	R_5	0	0	0

V. ADDITIONAL SYMMETRY AND LINE NODE

We now take into account other material-dependent symmetries that could stabilize a line node in odd-parity SCs. In particular, a line node can be invariant under reflection or spin rotation, which may yield an extra topological obstruction for opening a gap.

A. Reflection

For simplicity, assume that the reflection plane is perpendicular to the z axis. Then the reflection symmetry requires that

$$\tilde{M}H(k_x,k_y,k_z)\tilde{M}^\dagger = H(k_x,k_y,-k_z), \tag{9}$$

with $\tilde{M} = \mathrm{diag}(M,\eta_C^M M^*)$. The commutation relations between $\tilde{M}$ and C, T, and $\tilde{P}$ are defined by $\tilde{M}S = \eta_S^M S\tilde{M}$ ($S = C,T,\tilde{P}$), where $\eta_S^M = \pm 1$. Without loss of generality, we choose a phase of M such that $M^2 = -1$. The reflection can be a mirror reflection, which is a proper reflection in the presence of SOC, but the following arguments are applicable to any type of reflection.

We calculate the classifying space by adding $\tilde{M}$ in the underlying Clifford algebras, where $\tilde{M}$ satisfies $\{\gamma_z,\tilde{M}\} = [\gamma_{x,y},\tilde{M}] = 0$. As a result, the topological node stabilities under the reflection symmetry are obtained [Table II(A)], in which we specify η_S^M of $\tilde{M}$ by $M^{\eta_C^M\eta_P^M}$ for the P+D class and $M^{\eta_C^M\eta_P^M,\eta_C^M\eta_T^M}$ for the P+DIII class (see Appendix 2). For the single-band spin-triplet SC with TRS, the symmetry operations are given by $C = \tau_x K$, $T = i\sigma_y K$, and $\tilde{P} = \tau_z$, where τ_i and σ_i are the Pauli matrices describing the Nambu and spin spaces, respectively, and K represents the complex conjugate. Thus, mirror reflection with respect to the xy plane is labeled as M^{++} ($\tilde{M} = i\tau_z\sigma_z$) or M^{--} ($\tilde{M} = i\tau_0\sigma_z$). That is, a line node is unstable as Blount proved. Conversely, we provide counterexamples of the Blount's argument for the M^+ and M^{+-} cases [37]. The M^+ mirror reflection can be realized in a SC without TRS, whereas M^{+-} can be achieved in a SC with TRS if they have a particular normal state and multiband structures. This is shown in Appendix 3.

B. Spin rotation

For bulk Cooper pairs, the influence of SOC is strongly suppressed by the Fermi energy. Thus SRS exhibits approximate good symmetry. For convenience, we consider π-SRS such that $[H(\boldsymbol{k}),\tilde{U}] = 0$, where $\tilde{U} = \mathrm{diag}(U,\eta_C^U U^*)$ and $U^2 = -1$ [38]. We define the commutation relations between $\tilde{U}$ and C, T and $\tilde{P}$ by $\tilde{U}S = \eta_S^U S\tilde{U}$ and $\eta_S^U = \pm 1$ ($S = C,T,\tilde{P}$). Using the Clifford algebra extension method, the stability of nodes is calculated [Table II(B)], where we specify η_S^U by $U^{\eta_C^U\eta_P^U}$ for the P+D class and $U^{\eta_C^U\eta_P^U,\eta_C^U\eta_T^U}$ for the P+DIII class (see Appendix 2). From Table II(B), we find a stable line node in the U^{++} class. In the single-band spin-triplet SC with TRS, the π-SRS belongs to U^{++} or U^{--}. Thus the system may

TABLE II. Classification of nodes with IS and (A) reflection symmetry or (B) π-SRS. The fourth column of (A) and (B) lists the types of reflection symmetry and SRS classes, respectively. Here the superscripts of $M(U)$ represent the commutation relation with $C\tilde{P}$ and CT, i.e., $M^{\eta_C^M\eta_P^M}$ ($U^{\eta_C^U\eta_P^U}$) for the P+D class and $M^{\eta_C^M\eta_P^M,\eta_C^M\eta_T^M}$ ($U^{\eta_C^U\eta_P^U,\eta_C^U\eta_T^U}$) for the P+DIII class.

(A) PHS, TRS, IS (odd parity), and reflection symmetry							
Class	Symmetry	Parity	Reflection	$\mathcal{Q}$	$p=0$	$p=1$	$p=2$
P+D	$\{C\tilde{P},M\}$	Odd	M^+	R_7	0	$\mathbb{Z}$	$\mathbb{Z}_2$
			M^-	R_5	0	0	0
P+DIII	$\{C\tilde{P},T\tilde{P},M\}$	Odd	M^{++}	R_6	0	0	$\mathbb{Z}$
			M^{-+}	R_4	$2\mathbb{Z}$	0	0
			M^{+-}	C_1	0	$\mathbb{Z}$	0
			M^{--}	R_5	0	0	0

(B) PHS, TRS, IS (odd parity), and π-SRS							
Class	Symmetry	Parity	SRS	$\mathcal{Q}$	$p=0$	$p=1$	$p=2$
P+D	$\{C\tilde{P},\tilde{U}\}$	Odd	U^+	C_0	$\mathbb{Z}$	0	$\mathbb{Z}$
			U^-	R_6	0	0	$\mathbb{Z}$
P+DIII	$\{C\tilde{P},T\tilde{P},\tilde{U}\}$	Odd	U^{++}	C_1	0	$\mathbb{Z}$	0
			U^{-+}	R_5	0	0	0
			U^{+-}	R_4	$2\mathbb{Z}$	0	0
			U^{--}	R_6	0	0	$\mathbb{Z}$

support SRS-protected line nodes if U^{++}. It is noteworthy that the U^{++} class includes the polar phase in ^{3}He superfluid [1,3], in which the π-SRS is given by $\tilde{U} = i\tau_z\sigma_z$ when $\boldsymbol{d} \parallel \boldsymbol{z}$.

VI. SURFACE FLAT DISPERSION

Finally, we discuss the implications of our results. We first would like to mention that our results do not provide a strong constraint on the existence of bulk line nodes in odd-parity SCs. As mentioned above, SRS could exhibit good symmetry in the bulk. As such, for odd-parity SCs with TRS, SRS in the U^{++} class permits a topological stable bulk line node. Furthermore, even for those without TRS, the M^{+} reflection symmetry obtained by combining the mirror reflection with SRS allows for a stable bulk line node, as is seen in Table II(A). Nevertheless, our results do provide a strong implication for the corresponding surface states. The point is that the surface Rashba SOC, which breaks the SRS, cannot be neglected. The influence of the surface Rashba SOC is not suppressed by the Fermi energy; therefore the bulk-boundary correspondence does not hold for the SRS-protected line nodes in actual materials. Also, it should be noticed that IS, in general, breaks in a system with a boundary. However, the IS protected line nodes for even parity superconductors are topologically stable even without IS, the statement of which is shown in Appendix 4.

To illustrate the effect of the surface Rashba SOC, we numerically calculated the energy spectra for three-dimensional (3D) single-band odd-parity SCs with a gap function for the polar state [1] and E_{2u} state of the UPt_3 B phase [4], respectively. The normal state is given by $\epsilon(\boldsymbol{k}) = -2t(\cos k_x + \cos k_y + \cos k_z) - \mu$, where we assume a spherical Fermi surface, i.e., $\mu = -4t$. For the gap function, we consider $\Delta(\boldsymbol{k}) = \Delta_0 \sin k_z \sigma_x$ for the polar state [see Figs. 2(a) and 2(c)] and $\Delta(\boldsymbol{k}) = \Delta_0 \sin k_z(\cos k_x + 2i \sin k_x \sin k_y - \cos k_y)\sigma_x$ for the E_{2u} state of the UPt_3 B phase [see Figs. 2(b) and 2(d)]. For both cases, a line node exists on the $k_z = 0$ plane. Each line node is protected by U^{++}, as observed in Table II(B), and M^{+}, as observed in Table II(A) [39]. The system has an open boundary condition in the z direction and periodic boundary conditions for the x and y axes. In addition, we take into account the effect of the surface Rashba SOC as $\epsilon_R(\boldsymbol{k}) = \pm\lambda(\sin k_y\sigma_x - \sin k_x\sigma_y)$ for small distances from the open boundary, in which we take $+1(-1)$ for the top (bottom) surface. Numerically calculating the surface energy spectra, we obtain the zero-energy state in the absence of the surface Rashba SOC, which is shown by the black region in Figs. 2(a) and 2(b) [11,40,41]. However, once we take the surface Rashba SOC into account, nearly all the zero-energy states disappear for both gap functions [see Figs. 2(c) and 2(d)]. This is because the Rashba SOC breaks the SRS; namely, the line node is unstable under the Rashba SOC, and this instability generates a gap in a large region of the surface state. In contrast, the zero-energy surface flatbands in high-T_c cuprates or noncentrosymmetric SCs are stable under the surface Rashba SOC because the line nodes are only protected by TRS [11,15,16].

The instability of the zero-energy state in odd-parity SCs can be tested using tunneling spectroscopy because of the splitting or broadening the of zero-bias conductance peak, which provides a clear distinction from the sharp peak in high-T_c materials [34–36,42,43].

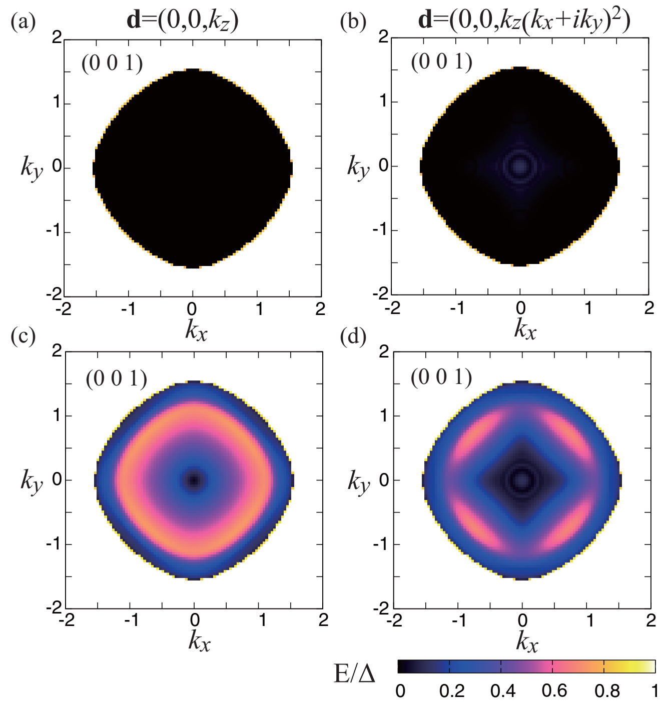

FIG. 2. (Color online) Energy spectra at the (001) face of the odd-parity SC with a line node as a function of surface momentum (k_x,k_y). $\mu = -4t$, $\Delta_0 = 0.3t$, and $\lambda = 0.3t$. The distance between upper ($z = L$) and lower ($z = 0$) surfaces is $L = 90$. For (a) and (c), $\boldsymbol{d} = \Delta_0(0,0,k_z)$, while for (b) and (d), $\boldsymbol{d} = \Delta_0[0,0,k_z(k_x + ik_y)^2]$. In (a) and (b), we ignore the Rashba SOC, whereas in (d) and (f), we include it in the distance $1 \leqslant z \leqslant 5$ and $85 \leqslant z \leqslant 90$. The color scale shows the energy. The black region represents a zero-energy state.

VII. SUMMARY AND DISCUSSION

We rebuilt the stability condition of line nodes in odd-parity SCs using the topological classification. The topological arguments update the Blount's theorem such that a line-node-associated flat zero-energy surface state is improbable in odd-parity SCs. Our updated Blount's theorem can be applied to various unconventional SCs such as UPt_3 [4], UBe_{13} [44], UNi_2Al_3 [45], and $Cu_xBi_2Se_3$ [46] because they are odd-parity SC candidates. Whereas a symmetry-protected line node was also proposed for nonsymmorphic odd-parity SCs [47], in which the line node is protected by twofold screw symmetry. Here the twofold screw operator is composed of a twofold rotation operator and a translation operator. The corresponding surface flat dispersion might disappears since any surface breaks the translation symmetry.

While we mainly focused on line nodes in odd-parity SCs, our classification is also applicable to other nodal structures. It is noteworthy that point nodes in the E_{1u} state of UPt_3 B phase [48] and $Cu_xBi_2Se_3$ [49,50] belong to the M^{++} class in Table II(A), and they are topologically stable.

Finally, we would like to mention that our method also works for Dirac materials such as graphene [51] and organic conductors [52]. For example, if we consider the TRS ($T^2 = 1$)

and inversion symmetry ($P^2 = 1$), a combined symmetry is TP ($[T,P] = 0$). By the same calculation with the SC state, we obtain $\mathcal{Q} = R_0$. The first homotopy group is $\pi_1(R_0) = \mathbb{Z}_2$, i.e., the Dirac cone is stable in two-dimensional systems such as graphene. Also, we can predict a stable Dirac cone in a 3D system because $\pi_2(R_0) = \mathbb{Z}_2$, which will provide a clue to novel topological materials.

ACKNOWLEDGMENTS

S.K. would like to thank A. Yamakage and K. Yada for their helpful comments. This work is supported in part by a Grant-in Aid for Scientific Research from MEXT of Japan, "Topological Quantum Phenomena," Grant No. 22103005 (M.S., Y.T.). S.K. acknowledges support from JSPS (Grant No. 256466). K.S. is supported by a JSPS Fellowship for Young Scientists. M.S. is supported by Grant-in-Aid for Scientific Research B (Grant No. 25287085) from JSPS.

APPENDIX

1. Stability of nodes and topological invariant

We discuss the connection between node stabilities and topological invariants. To be concrete, we consider a time-reversal invariant (TRI) superconductor without inversion symmetry. Assuming that a system is three dimensional and the Fermi surface is spherical, let us first consider a two-dimensional node, i.e., $\Delta(\boldsymbol{k}) = 0$ over the spherical Fermi surface. The BdG Hamiltonian is given by

$$H_{\mathrm{BdG}}(\boldsymbol{k}) = (\boldsymbol{k}^2/2m - \mu)\tau_z \otimes 1_{2\times2}, \tag{A1}$$

where m, μ, and $1_{2\times2}$ are a mass of electron, a chemical potential, and a 2×2 identity matrix, respectively. When we expand $H_{\mathrm{BdG}}(\boldsymbol{k})$ around a point $\boldsymbol{k}_0$ on the Fermi surface, the Hamiltonian close to the node is given by

$$H_{\boldsymbol{k}_0}(\boldsymbol{p}) := H_{\mathrm{BdG}}(\boldsymbol{k}_0 + \boldsymbol{p}) \simeq \boldsymbol{v}_0 \cdot \boldsymbol{p}\ \tau_z \otimes 1_{2\times2}, \tag{A2}$$

where $|\boldsymbol{p}| \ll 1$ and $\boldsymbol{v}_0 = \boldsymbol{k}_0/m$ ($|\boldsymbol{k}_0| = \sqrt{2m\mu}$). To make a superconducting gap on the Fermi surface, it is necessary to find a symmetry-preserving mass term (SPMT) denoted by γ_{M} [53,54], which is anticommute with $H_{\boldsymbol{k}_0}$. Since the underlying Hamiltonian has PHS $C = (\tau_x \otimes 1_{2\times2})K$ and TRS $T = (1_{2\times2} \otimes i\sigma_y)K$ and the node satisfies $\boldsymbol{k}_0 \neq -\boldsymbol{k}_0$, the SPMT has to satisfy $\{\gamma_{\mathrm{M}}, TC\} = 0$. We readily find the SPMT as $\gamma_M = \tau_y \otimes \sigma_y$. Thus the two-dimensional node (or gapless superconductor) is unstable.

Next, we consider the line node stability. The BdG Hamiltonian is given by

$$H_{\mathrm{BdG}}(\boldsymbol{k}) = (\boldsymbol{k}^2/2m - \mu)\tau_z \otimes 1_{2\times2} + v_\Delta k_z \tau_y \otimes 1_{2\times2}, \tag{A3}$$

where v_Δ is an amplitude of the gap function. There is the line node at $k_z = 0$ on the Fermi surface. The Hamiltonian close to the nodal point $\boldsymbol{k}_0 = (\sqrt{2m\mu}\cos\theta, \sqrt{2m\mu}\sin\theta, 0)$ is given by

$$H_{\boldsymbol{k}_0}(\boldsymbol{p}) = \boldsymbol{v}_0 \cdot \boldsymbol{p}\ \tau_z \otimes 1_{2\times2} + v_\Delta p_z \tau_y \otimes 1_{2\times2}. \tag{A4}$$

In this Hamiltonian, we cannot produce the superconducting gap due to the absence of the SPMT. Therefore the line node is stable.

As discussed above, the node stabilities are determined by the existence of the SPMT. In what follows, we show that the node stability relates to a topological invariant. For the sake of completeness, we restrict our attention to the TRI superconductor without inversion symmetry.

To see the topological invariant, we assume the Hamiltonian with a sufficiently large matrix dimension and regard the normal dispersion as a "mass term." Note that we define a mass term to characterize degrees of freedom of $H_{\boldsymbol{k}_0}$ based on Refs. [27–31], which is not a real mass term. In the case of the two-dimensional node, a $2N \times 2N$ Hamiltonian is given by

$$H_{\boldsymbol{k}_p}(\boldsymbol{p}) = \boldsymbol{v}_0 \cdot \boldsymbol{p}\ \tau_z \otimes 1_{N\times N}. \tag{A5}$$

The Hamiltonian has a chiral symmetry $\{H, TC\} = 0$. Now, we redefine $TC = \tau_x \otimes 1_{N\times N}$ for convenience sake. The general form of the Hamiltonian is given by

$$H'_{\boldsymbol{k}_p}(\boldsymbol{p}) = e^{i\tau_x\otimes A} e^{i\tau_0\otimes B}(\boldsymbol{v}_0 \cdot \boldsymbol{p}\ \tau_z \otimes 1_{N\times N}) e^{-i\tau_0\otimes B} e^{-i\tau_x\otimes A}, \tag{A6}$$

where A and B are $N \times N$ Hermitian matrices and $e^{i\tau_x\otimes A}e^{i\tau_0\times B} \in U(N) \times U(N)$. Here, we choose the Hamiltonian $H'_{\boldsymbol{k}_0}$ to remain the commutation relation with TC unchanged. Since $[e^{i\tau_0\times B}, H_{\boldsymbol{k}_p}] = 0$, the total degrees of freedom of $H'_{\boldsymbol{k}_0}$ are $U(N) \times U(N)/U(N) = U(N)$, which is the classifying space labeled by C_1. Since $U(N)$ is the connected space, $\pi_0[U(N)] = 0$, i.e., all of the mass terms are connected in terms of the unitary operation. This means that we can freely add the SPMT in H'_{k_p} and thus the Hamiltonian with the two-dimensional node continuously deforms to that with a full gap. This result is the same as the above argument of the SPMT.

Secondly, in the case of the line node, a $2N \times 2N$ Hamiltonian is given by

$$H_{\boldsymbol{k}_p}(\boldsymbol{p}) = \boldsymbol{v}_0 \cdot \boldsymbol{p}\ \tau_z \otimes D + v_\Delta p_z \tau_y \otimes 1_{N\times N}, \tag{A7}$$

where C represents normalized $N \times N$ Hermitian matrices ($D^2 = 1_{N\times N}$). The Hamiltonian $H_{\boldsymbol{k}_p}$ satisfies $\{H_{\boldsymbol{k}_0}, TC\} = 0$. Using an $N \times N$ unitary matrix $U_{N\times N} \in U(N)$, D is, in general, given by

$$D = U_{N\times N}\,\mathrm{diag}(1_{n\times n}, -1_{m\times m})U^\dagger_{N\times N}, \quad m + n = N. \tag{A8}$$

We readily see that D is invariant under $\mathrm{diag}(U_{n\times n}, U_{m\times m}) \in U(n) \times U(m)$. In addition, we have the freedom of choice about $m \in \mathbb{Z}$. Therefore the total degrees of freedom of the mass term is $\bigcup_m [U(n+m)/(U(n) \times U(m))]$. In the $N \to \infty$ limit, the classifying space becomes $[U(n+m)/(U(n) \times U(m))] \times \mathbb{Z}$, which is formally labeled by C_0. Since $\pi_0(C_0) = \mathbb{Z}$, the Hamiltonian with the line node cannot continuously transform into that with the gap. Thus the line node is topologically protected as discussed above. We summarize the classifying space C_q and R_q and the zeroth homotopy group of them at Table III. The higher homotopy groups are determined by the zeroth homotopy group because of the relations $\pi_p(C_i) = \pi_0(C_{i+p}) = \pi_0(C_{i+p+2})$ and $\pi_p(R_j) = \pi_0(R_{j+p}) = \pi_0(R_{j+p+8})$, where the last equalities come from the Bott periodicity [20].

TABLE III. Bott periodicity of the classifying space for (a) complex case C_q and (b) real case R_q. The last columns show the zeroth homotopy group of each classifying space.

(a) Complex case		
q mod 2	Classifying space C_q	$\pi_0(C_q)$
0	$[U(n+m)/U(n)\times U(m)]\times\mathbb{Z}$	$\mathbb{Z}$
1	$U(n)$	0
(b) Real case		
q mod 8	Classifying space R_q	$\pi_0(C_q)$
0	$[O(n+m)/O(n)\times O(m)]\times\mathbb{Z}$	$\mathbb{Z}$
1	$O(n)$	$\mathbb{Z}_2$
2	$O(2n)/U(n)$	$\mathbb{Z}_2$
3	$U(2n)/Sp(n)$	0
4	$[Sp(n+m)/Sp(n)\times Sp(m)]\times\mathbb{Z}$	$\mathbb{Z}$
5	$Sp(n)$	0
6	$Sp(n)/U(n)$	0
7	$U(n)/O(n)$	0

2. Clifford algebra extension method

In this section, we show the concrete calculation in Tables I and II in the main text. First, we briefly review a Clifford algebra extension method based on Refs. [20,29,30]. First, we define a set of complex Clifford algebras Cl_q, which has p generators satisfying

$$\{\gamma_i,\gamma_j\} = 2\delta_{ij} \quad (i,j=1,\dots p). \tag{A9}$$

On the other hand, a set of real Clifford algebras $Cl_{p,q}$ has p generators satisfying $\gamma_i^2=-1$ $(i=1,\dots,p)$ and q generators satisfying $\gamma_{p+j}^2=1$ $(j=1,\dots,q)$. The generators satisfy the commutation relation such that

$$\{\gamma_i,\gamma_j\}=0 \quad \text{if } i\neq j. \tag{A10}$$

For example, Cl_p and $Cl_{p,q}$ are equivalent to the following algebras:

$$Cl_0=\mathbb{C},\quad Cl_1=\mathbb{C}\oplus\mathbb{C} \tag{A11}$$

and

$$\begin{aligned} &Cl_{0,0}=\mathbb{R},\quad Cl_{1,0}=\mathbb{C},\quad Cl_{0,1}=\mathbb{R}\oplus\mathbb{R},\\ &Cl_{2,0}=\mathbb{H},\quad Cl_{0,2}=\mathbb{R}(2),\end{aligned} \tag{A12}$$

where $\mathbb{H}$ is a quaternion and $\mathbb{R}(2)$ is a 2×2 real matrix. We note that "=" represents isomorphism on the algebra. In addition, we have some properties on $Cl_{p,q}$, which is useful to discuss the extension problem, as follows:

$$Cl_{q,p+2}=Cl_{p,q}\otimes Cl_{0,2}, \tag{A13}$$

$$Cl_{q+2,p}=Cl_{p,q}\otimes Cl_{2,0}, \tag{A14}$$

$$Cl_{p+1,q+1}=Cl_{p,q}\otimes Cl_{1,1}, \tag{A15}$$

$$Cl_{p,q+8}=Cl_{p,q}\otimes Cl_{0,8},=Cl_{p,q}\otimes\mathbb{R}(16), \tag{A16}$$

$$Cl_{p+q}=Cl_{p,q}\otimes Cl_{1,0}=Cl_{p,q}\otimes_{\mathbb{R}}\mathbb{C}, \tag{A17}$$

$$Cl_{p+2}=Cl_p\otimes\mathbb{C}(2), \tag{A18}$$

where $\mathbb{R}(16)$ and $\mathbb{C}(2)$ are a 16×16 real matrix and a 2×2 complex matrix, respectively.

TABLE IV. Relationship between the symmetry class, the Clifford algebra extension, and the classifying space in the system with inversion symmetry. The first, second, and third columns show the symmetry class, the symmetry constraints, and the parity of gap functions, respectively. The fourth and fifth columns show the Clifford algebra extensions and the corresponding classifying spaces.

Class	Symmetry	Parity	Extension	Classifying space
D	$\{1\}$	N/A	$Cl_p\to Cl_{p+1}$	C_p
DIII	$\{TC\}$	N/A	$Cl_{p+1}\to Cl_{p+2}$	C_{p+1}
P+D	$\{C\tilde{P}\}$	Even	$Cl_{0,p+2}\to Cl_{0,p+3}$	R_{p+2}
		Odd	$Cl_{2,p}\to Cl_{2,p+1}$	R_{p-2}
P+DIII	$\{C\tilde{P},T\tilde{P}\}$	Even	$Cl_{0,p+3}\to Cl_{0,p+4}$	R_{p+3}
		Odd	$Cl_{3,p}\to Cl_{3,p+1}$	R_{p-3}

The Clifford algebra extension method leads the classifying space systematically. The relationship between the Clifford algebra extension and the classifying space is summarized as follows:

$$Cl_p\to Cl_{p+1}\ \Leftrightarrow\ C_p, \tag{A19}$$

$$Cl_{p,q}\to Cl_{p,q+1}\ \Leftrightarrow\ R_{q-p}, \tag{A20}$$

$$Cl_{p,q}\to Cl_{p+1,q}\ \Leftrightarrow\ R_{p+2-q}, \tag{A21}$$

where the left-hand side of Eqs. (A19)–(A21) represents the Clifford algebra extension and the right-hand side of these is the corresponding classifying spaces. The last equation (A21) is derived from Eq. (A20) by using the property (A13). Also, we can confirm the Bott periodicity for both the real and complex representations by utilizing the property (A16) and (A18), since $\mathbb{R}(16)$ and $\mathbb{C}(2)$ do not affect in the extension for each representation.

We show concrete calculations of the Clifford algebra extension method in the system with inversion symmetry, reflection symmetry, and π-SRS at Tables IV, V, and VI. For example, in the P+D class with odd parity, i.e., $(C\tilde{P})^2=-1$, the Hamiltonian of a $(p+1)$-codimensional node is given by

$$H_{\boldsymbol{k}_0}(\boldsymbol{p})=\sum_{i=1}^{p+1}k_i\gamma_i, \tag{A22}$$

which satisfies $\{H_{\boldsymbol{k}_0},C\tilde{P}\}=0$. In addition, we introduce a "complex structure" J $(J^2=-1)$, which is anticommutative with $C\tilde{P}$ and is commutative with $H_{\boldsymbol{k}_0}$. To see the classifying space of $H_{\boldsymbol{k}_0}$, we regard γ_{p+1} as a "mass term." As a result, the Clifford algebras extension is given by $\{\gamma_1,\dots,\gamma_p,C\tilde{P},JC\tilde{P}\}\to\{\gamma_1,\dots,\gamma_p,\gamma_{p+1},C\tilde{P},JC\tilde{P}\}$, where $\{\dots\}$ represents a set of the Clifford algebras satisfying Eq. (A10). This extension means that $Cl_{2,p}\to Cl_{2,p+1}$, so the classifying space is R_{p-2} by Eq. (A20). Also, the topological invariant is given by $\pi_0(R_{p-2})=\pi_0(R_{p-2+8})=\pi_p(R_6)$.

When the Hamiltonian (A22) has a reflection symmetry $\tilde{M}$ $(\tilde{M}^2=-1)$ additionally, we need to modify this extension problem. We assume $\{\gamma_1,\tilde{M}\}=[\gamma_{i\neq 1},\tilde{M}]=[J,\tilde{M}]=0$ so that the reflection affects k_1 as $k_1\to -k_1$, i.e., k_1 is momentum transverse to the reflection plane and a

TABLE V. Relationship between the symmetry class, the Clifford algebra extension, and the classifying space in the system with inversion symmetry and reflection symmetry. The fourth column represents the mirror classes, in which a superscript means a commutation relation with C, T, and $\tilde{P}$, i.e., $M^{\eta_C^M\eta_P^M}$ for the P+D class and $M^{\eta_C^M\eta_P^M,\eta_C^M\eta_T^M}$ for the P+DIII class, respectively. The fifth and sixth columns show the Clifford algebra extensions and the corresponding classifying spaces for each mirror class.

Class	Symmetry	Parity	Mirror	Extension	Classifying space
P+D	$\{C\tilde{P},\tilde{M}\}$	Odd	M^+	$Cl_{2,p+1}\to Cl_{2,p+2}$	R_{p-1}
			M^-	$Cl_{3,p}\to Cl_{3,p+1}$	R_{p-3}
P+DIII	$\{C\tilde{P},T\tilde{P},\tilde{M}\}$	Odd	M^{++}	$Cl_{3,p+1}\to Cl_{3,p+2}$	R_{p-2}
			M^{-+}	$Cl_{4,p}\to Cl_{4,p+1}$	R_{p-4}
			M^{+-}	$Cl_{p+3}\to Cl_{p+4}$	C_{p+3}
			M^{--}	$Cl_{3,p}\to Cl_{3,p+1}$	R_{p-3}

node lies on the reflection symmetric subspace. The Clifford algebra extension depends on whether the reflection symmetry commutes or anticommutes with $C\tilde{P}$. When $[C\tilde{P},\tilde{M}]=0$ (M^+ class), the Clifford algebra extension is given by $\{\gamma_1,\dots,\gamma_p,C\tilde{P},JC\tilde{P},\gamma_1\tilde{M}\}\to\{\gamma_1,\dots,\gamma_p,\gamma_{p+1},C\tilde{P},JC\tilde{P},\gamma_1\tilde{M}\}$. Hence, the classifying space is R_{p-1}. On the other hand, when $\{C\tilde{P},\tilde{M}\}=0$ (M^- class), the Clifford algebra extension is given by $\{\gamma_1,\dots,\gamma_p,C\tilde{P},JC\tilde{P},J\gamma_1\tilde{M}\}\to\{\gamma_1,\dots,\gamma_p,\gamma_{p+1},C\tilde{P},JC\tilde{P},J\gamma_1\tilde{M}\}$. That is, the classifying space is R_{p-3}. By repeating the same calculation for each case, we obtain Tables IV and V.

Finally, we discuss the Hamiltonian with π-SRS $\tilde{U}$, where $\tilde{U}^2=-1$ and $[\gamma_i,\tilde{U}]=[J,\tilde{U}]=0$ ($i=1,2,\dots,p+1$). The Clifford algebra extension depends on either $[C\tilde{P},\tilde{U}]=0$ or $\{C\tilde{P},\tilde{U}\}=0$ in the P+D class. They are labeled by U^+ and U^-, respectively. The Clifford algebra extension for each case is given by $\{\gamma_1,\dots,\gamma_p,C\tilde{P},JC\tilde{P}\}\otimes\{\tilde{U}\}\to\{\gamma_1,\dots,\gamma_p,\gamma_{p+1},C\tilde{P},JC\tilde{P}\}\otimes\{\tilde{U}\}$ in the U^+ class and $\{\gamma_1,\dots,\gamma_p,C\tilde{P},JC\tilde{P}\}\otimes\{J\tilde{U}\}\to\{\gamma_1,\dots,\gamma_p,\gamma_{p+1},C\tilde{P},JC\tilde{P}\}\otimes\{J\tilde{U}\}$ in the U^- class. Here, $\{A\}\otimes\{B\}$ means that A and B are commutative to each other. In the former case, the classifying space is C_{p+2}, since $\tilde{U}$ gives the complex structure by Eq. (A17), whereas the latter shows the classifying space R_{p-2}, since $J\tilde{U}$ just block diagonalizes $H_{\boldsymbol{k}_0}$, which has no effect on the classification. In the P+DIII class, we need to include the symmetry $T\tilde{P}$ in the underlying Clifford algebra. For instance, in the U^{++} class, the Clifford algebra extension is given by $\{\gamma_1,\dots,\gamma_p,C\tilde{P},JC\tilde{P},CT\}\otimes\{\tilde{U}\}\to\{\gamma_1,\dots,\gamma_p,\gamma_{p+1},C\tilde{P},JC\tilde{P},CT\}\otimes\{\tilde{U}\}$. Hence, the classifying space is C_{p+3}, since $\tilde{U}^2=-1$. By repeating the same calculation for the other classes, we obtain Table VI. To complete the node stabilities under inversion symmetry, we also show the topological node stabilities under reflection symmetry and π-SRS in the even-parity case [see Tables VII(C) and VII(D)].

3. Examples for the M^+ and M^{+-} classes

As seen in Table II(A), a stable line node is allowed for the M^+ and M^{+-} classes, which are conflict with the original Blount's argument. In this section, we show that the stability of the line node comes from that of the Fermi surface intersecting with the reflection plane. In what follows, we construct the concrete BdG Hamiltonians belonging to the M^+ class and the M^{+-} class.

First, we discuss the M^+ class. The corresponding BdG Hamiltonian is given by

$$H(\boldsymbol{k})=\begin{pmatrix}\epsilon(\boldsymbol{k})-\mu-h\sigma_z & iv_\Delta k_z\\ -iv_\Delta k_z & -\epsilon(\boldsymbol{k})+\mu+h\sigma_z\end{pmatrix},\qquad (A23)$$

where h is a magnetic field of the z direction that breaks TRS. The PHS, the inversion symmetry, and the reflection

TABLE VI. Relationship between the symmetry class, the Clifford algebra extension, and the classifying space in the system with inversion symmetry and SRS. The fourth column represents the SRS classes, in which a superscript means a commutation relation with C, T, and $\tilde{P}$, i.e., $U^{\eta_C^U\eta_P^U}$ for the P+D class and $M^{\eta_C^U\eta_P^U,\eta_C^U\eta_T^U}$ for the P+DIII class, respectively. The fifth and sixth columns show the Clifford algebra extensions and the corresponding classifying spaces for each SRS class.

Class	Symmetry	Parity	SRS	Extension	Classifying space
P+D	$\{C\tilde{P},\tilde{U}\}$	Odd	U^+	$Cl_{p+2}\to Cl_{p+3}$	C_{p+2}
			U^-	$Cl_{2,p}\to Cl_{2,p+1}$	R_{p-2}
P+DIII	$\{C\tilde{P},T\tilde{P},\tilde{U}\}$	Odd	U^{++}	$Cl_{p+3}\to Cl_{p+4}$	C_{p+3}
			U^{-+}	$Cl_{3,p}\to Cl_{3,p+1}$	R_{p-3}
			U^{+-}	$Cl_{4,p}\to Cl_{4,p+1}$	R_{p-4}
			U^{--}	$Cl_{3,p+1}\to Cl_{3,p+2}$	R_{p-2}

TABLE VII. Classification of nodes with IS (even parity) and (C) reflection symmetry or (D) π-SRS. The fourth column of (C) and (D) list the types of reflection symmetry and SRS classes, respectively. Here the superscripts of $M(U)$ represent the commutation relation with $C\tilde{P}$ and CT, i.e., $M^{\eta_C^M \eta_P^M}(U^{\eta_C^U \eta_P^U})$ for the P+D class and $M^{\eta_C^M \eta_P^M,\eta_C^M \eta_T^M}(U^{\eta_C^U \eta_P^U,\eta_C^U \eta_T^U})$ for the P+DIII class. The fifth and sixth columns show the Clifford algebra extensions and the corresponding classifying spaces, respectively. The following columns represent the topological number for each reflection and SRS class.

(C) PHS, TRS, IS (even parity), and reflection symmetry								
Class	Symmetry	Parity	Reflection	Extension	Classifying space	$p=0$	$p=1$	$p=2$
P+D	$\{C\tilde{P},M\}$	Even	M^+	$Cl_{0,p+3}\to Cl_{0,p+4}$	R_{p+3}	0	$2\mathbb{Z}$	0
			M^-	$Cl_{1,p+2}\to Cl_{1,p+3}$	R_{p+1}	$\mathbb{Z}_2$	$\mathbb{Z}_2$	0
P+DIII	$\{C\tilde{P},T\tilde{P},M\}$	Even	M^{++}	$Cl_{0,p+4}\to Cl_{0,p+5}$	R_{p+4}	$2\mathbb{Z}$	0	0
			M^{-+}	$Cl_{1,p+3}\to Cl_{1,p+4}$	R_{p+2}	$\mathbb{Z}_2$	0	$2\mathbb{Z}$
			M^{+-}	$Cl_{0,p+3}\to Cl_{0,p+4}$	R_{p+3}	0	$2\mathbb{Z}$	0
			M^{--}	$Cl_{p+3}\to Cl_{p+4}$	C_{p+1}	0	$\mathbb{Z}$	0
(D) PHS, TRS, IS (even parity), and π-SRS								
Class	Symmetry	Parity	SRS	Extension	Classifying space	$p=0$	$p=1$	$p=2$
P+D	$\{C\tilde{P},\tilde{U}\}$	Even	U^+	$Cl_{p+2}\to Cl_{p+3}$	C_p	$\mathbb{Z}$	0	$\mathbb{Z}$
			U^-	$Cl_{0,p+2}\to Cl_{0,p+3}$	R_{p+2}	$\mathbb{Z}_2$	0	$2\mathbb{Z}$
P+DIII	$\{C\tilde{P},T\tilde{P},\tilde{U}\}$	Even	U^{++}	$Cl_{p+3}\to Cl_{p+4}$	C_{p+1}	0	$\mathbb{Z}$	0
			U^{-+}	$Cl_{0,p+3}\to Cl_{0,p+4}$	R_{p+3}	0	$2\mathbb{Z}$	0
			U^{+-}	$Cl_{0,p+4}\to Cl_{0,p+5}$	R_{p+4}	$2\mathbb{Z}$	0	0
			U^{--}	$Cl_{1,p+3}\to Cl_{1,p+4}$	R_{p+2}	$\mathbb{Z}_2$	0	$2\mathbb{Z}$

symmetry are given by $C=(\tau_x\otimes 1_{2\times 2})K$, $\tilde{P}=\tau_z\otimes 1_{2\times 2}$, and $\tilde{M}_{xy}=\tau_z\otimes i\sigma_z$, respectively. From the definition, the symmetries satisfy $[C\tilde{P},\tilde{M}]=0$ and the Hamiltonian (A23) has the line node at $k_z=0$ on the Fermi surface. On the mirror plane, i.e., $k_z=0$, the Hamiltonian is block diagonalized by $\tilde{M}_{xy}$, whose eigenvalues are given by $\pm i$. Thus, the matrix (A23) is decomposed into the mirror sector labeled by $H^{(+i)}$ and $H^{(-i)}$ such as

$$H(k_x,k_y,k_z=0) = H^{(+i)}(k_x,k_y,k_z=0)\oplus H^{(-i)}(k_x,k_y,k_z=0), \quad \text{(A24)}$$

where

$$H^{(\pm i)}=\pm\begin{pmatrix}\epsilon(\boldsymbol{k})-\mu-h & 0\\ 0 & -\epsilon(\boldsymbol{k})+\mu-h\end{pmatrix}. \quad \text{(A25)}$$

Since $H^{(+i)}$ and $H^{(-i)}$ have the same structure, we only consider the $+i$ sector. The upper left and lower right elements of (A25) represent the Fermi surface of the spin up and the spin down, respectively. When $h>\mu$, the Fermi surface of the spin-down component vanishes, since $-\epsilon(\boldsymbol{k})+\mu-h=0$ does not have a real solution. [Note that $\epsilon(\boldsymbol{k})=\boldsymbol{k}^2/2m$]. In such a situation, there is no mixing term which opens a gap in the Fermi surface of the spin-up component in the $+i$ sector. Thus the line node is stable.

Second, we consider the M^{+-} class. The corresponding BdG Hamiltonian is given by

$$H(\boldsymbol{k})=\begin{pmatrix}\epsilon(\boldsymbol{k})-\mu-\lambda\sigma_z\otimes s_x & iv_\Delta k_z\\ -iv_\Delta k_z & -\epsilon(\boldsymbol{k})+\mu+\lambda\sigma_z\otimes s_x\end{pmatrix}, \quad \text{(A26)}$$

where s_i $(i=x,y,z)$ is additional degrees of freedom such as an orbital and λ is a coupling constant between σ_z and s_x. The PHS, the TRS, the inversion symmetry, and the reflection symmetry are given by $C=(\tau_x\otimes 1_{4\times 4})K$, $T=(1_{2\times 2}\otimes i\sigma_y\otimes s_z)K$, $\tilde{P}=\tau_z\otimes 1_{4\times 4}$, and $\tilde{M}_{xy}=\tau_z\otimes i\sigma_z\otimes s_x$, respectively. From the definition, the symmetries satisfy $[C\tilde{P},\tilde{M}]=\{TC,\tilde{M}\}=0$, and the Hamiltonian (A26) has the line node at $k_z=0$ on the Fermi surface. Since $\tilde{M}^2=-1$, $H(k_x,k_y,k_z=0)$ is similarly decomposed into 4×4 matrices: $H^{(+i)}$ and $H^{(-i)}$. These are given by

$$H^{(\pm i)}=\pm\begin{pmatrix}\epsilon(\boldsymbol{k})-\mu-\lambda & 0 & 0 & 0\\ 0 & \epsilon(\boldsymbol{k})-\mu-\lambda & 0 & 0\\ 0 & 0 & -\epsilon(\boldsymbol{k})+\mu-\lambda & 0\\ 0 & 0 & 0 & -\epsilon(\boldsymbol{k})+\mu-\lambda\end{pmatrix}, \quad \text{(A27)}$$

where the basis of $H^{(+i)}$ is $1/\sqrt{2}(c_{\boldsymbol{k},\uparrow 1}+c_{\boldsymbol{k},\uparrow 2},-c_{\boldsymbol{k},\downarrow 1}+c_{\boldsymbol{k},\downarrow 2},-c^\dagger_{-\boldsymbol{k},\uparrow 1}+c^\dagger_{-\boldsymbol{k},\uparrow 2},c^\dagger_{-\boldsymbol{k},\downarrow 1}+c^\dagger_{-\boldsymbol{k},\downarrow 2})$. The subscripts $\uparrow$ $(\downarrow)$ and 1(2) represent the spin and the additional degrees of freedom, respectively. When $\lambda>\mu$, the Fermi surface of the electronic states $1/\sqrt{2}(-c_{\boldsymbol{k},\uparrow 1}+c_{\boldsymbol{k},\uparrow 2},c_{\boldsymbol{k},\downarrow 1}+c_{\boldsymbol{k},\downarrow 2})$ becomes unstable. In such a situation, Eq. (A27) does not have any mixing term which produces a gap, so the line node is stable.

4. Zero-energy state and inversion-symmetry-protected line node

In this section, we discuss how inversion-symmetry-protected nodes behave when inversion symmetry is absent. In particular, we argue that an inversion-symmetry-protected line nodes for even parity superconductors generate zero-energy flat dispersion at a certain surface. In the preceding study, the relation between a line node, which is protected by TRS, and a surface-zero-energy state has been established in Refs. [11,14]. Thus, we presume that the bulk-boundary correspondence exists in the D and DIII classes. We here construct a map from the P+D (P+DIII) class to the D (DIII) class, namely, we discuss the topological stability of a line node when we omit the inversion symmetry in the underlying BdG Hamiltonian. In what follows, we split the main statement into the four statements, (a), (b), (c), and (d), to complete all of the classes in Table I and II in the main text.

First of all, we show that (a) *a node is unstable in the D (DIII) class if the node is unstable in the P+D (P+DIII) class*. To see this, we use the following equivalent statements:

(1) A topological invariant does not exist.

(2) There exists a mass term, which preserves symmetries and is anticommutative with $H_{\boldsymbol{k}_0}$.

(3) A node is unstable.

To show (a), we assume that there exists a mass term γ_M ($[J,\gamma_M]=0$) in the P+D class such that

$$\{C\tilde{P},\gamma_M\}=\{H_{\boldsymbol{k}_0},\gamma_M\}=0. \qquad \text{(A28)}$$

Also, in the P+DIII class, there exists the mass term satisfying the following conditions:

$$\{C\tilde{P},\gamma_M\}=[T\tilde{P},\gamma_M]=\{H_{\boldsymbol{k}_0},\gamma_M\}=0. \qquad \text{(A29)}$$

Alternatively, Eq. (A29) is written by

$$\{C\tilde{P},\gamma_M\}=\{CT,\gamma_M\}=\{H_{\boldsymbol{k}_0},\gamma_M\}=0. \qquad \text{(A30)}$$

Equations (A28) and (A30) imply that the mass term always makes a gap in the underlying Hamiltonian with and without inversion symmetry. Namely, γ_M is the mass term in the D (DIII) class as well.

Second, we show that (b) *when the classifying space becomes the complex class by adding an additional symmetry, a node is stable in the D (DIII) class if the node is stable in the P+D (P+DIII) class*. The proof of this statement consists of three steps: (b-1) We derive conditions of an additional symmetry U which is required to become the complex class. (b-2) Both the D and the P+D classes are topologically nontrivial when p is even. Similarly, both the DIII and the P+DIII classes are topologically nontrivial when p is odd. (b-3) Under the map f, which omits the inversion symmetry in the underlying Hamiltonian, a topologically nontrivial Hamiltonian of the P+D (P+DIII) class is mapped into that of the D (DIII) class when p is even (odd).

In the step (b-1), the additional symmetry U is defined by

$$\{U,\gamma_i\}=[U,\gamma_{j\neq i}]=[U,J]=0 \quad (i=1,2,\ldots,m), \quad \text{(A31)}$$

where $U^2=\epsilon_U$ and $\epsilon_U=\pm 1$. Then the condition to become the complex class is directly derived from the Clifford algebra extension method; the results are given by

(1) P+D class

(i) $[C\tilde{P},U]=0$ and m is even, where m satisfies $(-1)^{\frac{m(m+1)}{2}}\epsilon_U=-1$.

(ii) $\{C\tilde{P},U\}=0$ and m is even, where m satisfies $(-1)^{\frac{m(m+1)}{2}}\epsilon_U=+1$.

(2) P+DIII class

(iii) $[C\tilde{P},U]=[TC,U]=0$ and m is even, where m satisfies $(-1)^{\frac{m(m+1)}{2}}\epsilon_U=-1$.

(iv) $\{C\tilde{P},U\}=[TC,U]=0$ and m is even, where m satisfies $(-1)^{\frac{m(m+1)}{2}}\epsilon_U=+1$.

(v) $[C\tilde{P},U]=\{TC,U\}=0$ and m is odd, where m satisfies $(-1)^{\frac{(m+1)(m+2)}{2}}\epsilon_U\epsilon_{CT}=-1$.

(vi) $\{C\tilde{P},U\}=\{TC,U\}=0$ and m is odd, where m satisfies $(-1)^{\frac{(m+1)(m+2)}{2}}\epsilon_U\epsilon_{CT}=+1$,

The factor ϵ_{CT} is defined by $(CT)^2=\epsilon_{CT}=\pm 1$. Note that the reflection symmetry and the π-SRS correspond to $m=1$ and $m=0$, respectively. Hence, the M^{+-} class belongs to the case (v), whereas the U^{+} and the U^{++} classes belong to cases (i) and (iii), respectively.

From the calculation of the step (b-1), the "complex structure" U' of cases (i)–(vi), i.e., U' is commutative with all underlying Clifford algebras, is given by (i),(iii) $U'=\gamma_1\cdots\gamma_m U$, (ii),(iv) $U'=J\gamma_1\cdots\gamma_m U$, (v) $U'=CT\gamma_1\cdots\gamma_m U$, and (vi) $U'=JCT\gamma_1\cdots\gamma_m U$, respectively.

Next, to prove step (b-2), we relate the P+D (P+DIII) class to the D (DIII) class. This is accomplished by defining a map f, which omits the inversion symmetry $\tilde{P}$ in the underlying symmetries. In the P+D class, the map f is given by

$$\begin{aligned} f:\{\gamma_1,\ldots,\gamma_{p+1},JC\tilde{P},CP\}\otimes\{U'\} \\ \to\{\gamma_1,\ldots,\gamma_{p+1}\}\otimes\{U'\}. \end{aligned} \qquad \text{(A32)}$$

Since the system always belongs to the complex class, the classifying spaces are C_{p+2} in the P+D class and C_p in the D class. Thus the classifying space is invariant under the map f due to the Bott periodicity. In the same fashion, in the P+DIII class, the map f is defined by

$$\begin{aligned} f:\{\gamma_1,\ldots,\gamma_{p+1},JC\tilde{P},C\tilde{P},CT\}\otimes\{U'\} \\ \to\{\gamma_1,\ldots,\gamma_{p+1},CT\}\otimes\{U'\}. \end{aligned} \qquad \text{(A33)}$$

The classifying spaces are C_{p+3} in the P+DIII class and C_{p+1} in the DIII class; i.e., the classifying space remains unchanged under the map f. As a result, step (b-2) is confirmed.

Finally, to show step (b-3), we construct topologically nontrivial Dirac Hamiltonians of the cases (i)–(vi), which have no SPMT. We describe the Dirac Hamiltonians concretely as follows:

(1) Dirac Hamiltonian of cases (i) and (ii)

We assume without a loss of generality that $m=0$ and $(C\tilde{P})^2=-1$. The Dirac Hamiltonians of case (i) are given by

$$H_0=k_1\tau_x,\quad C\tilde{P}=i\tau_y K,\quad U=i\tau_x,$$
$$H_2=H_0\otimes\sigma_x+k_2 1_{2\times 2}\otimes\sigma_y+k_3\tau_x\otimes\sigma_z,$$

$$
\begin{aligned}
C\tilde{P} &= (i\tau_y \otimes 1_{2\times 2})K, \quad U = i\tau_x \otimes 1_{2\times 2},\\
&\vdots\\
H_{2n} &= H_{2n-2}\otimes l_x + k_{2n}1_{2n\times 2n}\otimes l_y\\
&\quad + k_{2n+1}\tau_x\otimes 1_{2n-2\times 2n-2}\otimes l_z,\\
C\tilde{P} &= (i\tau_y\otimes 1_{2n\times 2n})K, \quad U = i\tau_x\otimes 1_{2n\times 2n}, \qquad \text{(A34)}
\end{aligned}
$$

where τ_i, σ_i, and l_i ($i = x,y,z$) are Pauli matrices, respectively. Similarly, we obtain case (ii) by replacing $U = i\tau_x \otimes 1_{2n\times 2n}$ with $U = \tau_x \otimes 1_{2n\times 2n}$.

(2) Dirac Hamiltonian of cases (iii) and (iv)

We assume without a loss of generality that $m = 0$, $(C\tilde{P})^2 = -1$ and $(CT)^2 = 1$. The Dirac Hamiltonians of case (iii) are given by

$$
\begin{aligned}
H_1 &= k_1\tau_x\otimes\sigma_x + k_2\tau_x\otimes\sigma_z,\\
C\tilde{P} &= (i\tau_y\otimes 1_{2\times 2})K,\\
U &= i\tau_x\otimes 1_{2\times 2}, \quad CT = 1_{2\times 2}\otimes\sigma_y,\\
H_3 &= H_1\otimes s_x + k_3 1_{4\times 4}\otimes s_y + k_4\tau_x\otimes 1_{2\times 2}\otimes s_z,\\
C\tilde{P} &= (i\tau_y\otimes 1_{4\times 4})K,\\
U &= i\tau_x\otimes 1_{4\times 4}, \quad CT = 1_{2\times 2}\otimes\sigma_y\otimes s_x,\\
&\vdots\\
H_{2n+1} &= H_{2n-1}\otimes l_x + k_{2n+1}1_{2n+2\times 2n+2}\otimes l_y\\
&\quad + k_{2n+2}\tau_x\otimes 1_{2n\times 2n}\otimes l_z,\\
C\tilde{P} &= (i\tau_y\otimes 1_{2n+2\times 2n+2})K,\\
U &= i\tau_x\otimes 1_{2n+2\times 2n+2},\\
CT &= 1_{2\times 2}\otimes\sigma_y\otimes s_x\otimes\cdots\otimes l_x, \qquad \text{(A35)}
\end{aligned}
$$

where τ_i, σ_i, s_i, and l_i ($i = x,y,z$) are Pauli matrices, respectively. Case (iv) is given by replacing $U = i\tau_x\otimes 1_{2n\times 2n}$ with $U = \tau_x \otimes 1_{2n\times 2n}$.

(3) Dirac Hamiltonian of cases (v) and (vi)

We assume without a loss of generality that $m = 1$, $(C\tilde{P})^2 = -1$, and $(CT)^2 = 1$. The Dirac Hamiltonians of case (vi) are given by

$$
\begin{aligned}
H_1 &= k_1\tau_x\otimes\sigma_x + k_2\tau_x\otimes\sigma_z,\\
C\tilde{P} &= (i\tau_y\otimes 1_{2\times 2})K,\\
U &= i1_{2\times 2}\otimes i\sigma_z,\\
CT &= 1_{2\times 2}\otimes\sigma_y,\\
H_3 &= H_1\otimes s_x + k_3 1_{4\times 4}\otimes s_y + k_4\tau_x\otimes 1_{2\times 2}\otimes s_z,\\
C\tilde{P} &= (i\tau_y\otimes 1_{4\times 4})K,\\
U &= 1_{2\times 2}\otimes i\sigma_z\otimes 1_{2\times 2},\\
CT &= 1_{2\times 2}\otimes\sigma_y\otimes s_x,\\
&\vdots\\
H_{2n+1} &= H_{2n-1}\otimes l_x + k_{2n+1}1_{2n+2\times 2n+2}\otimes l_y\\
&\quad + k_{2n+2}\tau_x\otimes 1_{2n\times 2n}\otimes l_z,\\
C\tilde{P} &= (i\tau_y\otimes 1_{2n+2\times 2n+2})K,\\
U &= 1_{2\times 2}\otimes i\sigma_z\otimes 1_{2n-2\times 2n-2},\\
CT &= 1_{2\times 2}\otimes\sigma_y\otimes s_x\otimes\cdots\otimes l_x, \qquad \text{(A36)}
\end{aligned}
$$

where τ_i, σ_i, s_i, and l_i ($i = x,y,z$) are Pauli matrices, respectively. Case (v) is given by the same Dirac Hamiltonian with $U = 1_{2\times 2}\otimes\sigma_z\otimes 1_{2n-2\times 2n-2}$. Note that the general forms of Eqs. (A34), (A35), and (A36) are achieved by acting a unitary operation due to the uniqueness of the Clifford algebras.

As described the above, the higher-dimensional Dirac Hamiltonian is inductively derived by the lowest-dimensional one. The higher-dimensional Dirac Hamiltonian of (i)–(vi) does not have a mass term with or without the inversion symmetry $\tilde{P}$ if there is no mass term in the lowest-dimensional one by the property of Pauli matrices. Thus we focus only on the lowest-dimensional one. In case (i), when we omit the inversion symmetry $\tilde{P}$ in the Hamiltonian H_0, the Dirac Hamiltonian and the symmetry become

$$H_0 = k_1\tau_x, \quad U = i\tau_x. \qquad \text{(A37)}$$

Obviously, there is no mass term satisfying $\{H_0,\gamma_M\} = [U,\gamma_M] = 0$ in Eq. (A37). Thus a topologically nontrivial Hamiltonian of the P+D class is mapped to that of the D class. In a similar way, we can verify the absence of the mass term under the map f in the lowest-dimensional Hamiltonian of the cases (ii)–(vi). As a result, the statement (b) is confirmed.

Finally, we show that (c) *a line node is stable in the D class with reflection symmetry if the line node is stable in the* M^+ *class* and (d) *a line node is stable in the DIII class if the line node is stable in the P+DIII with even parity*. In what follows, we attack the statements (c) and (d) individually.

For the case of (c), the M^+ class has the topologically stable line node as shown in Table II(A), whereas the D class with reflection symmetry also has the topological stable line node since $\mathcal{Q} = C_1$ and $\pi_1(C_1) = \mathbb{Z}$. In this case, we can construct the map from a topological nontrivial Hamiltonian of the M^+ class to that of the D class with reflection symmetry. To see this, we create the Dirac model of M^+ class as follows:

$$
\begin{aligned}
H_1 &= k_1\tau_z\otimes\sigma_x + k_2\tau_z\otimes\sigma_z,\\
C\tilde{P} &= (i\tau_y\otimes 1_{2\times 2})K, \qquad \text{(A38)}\\
\tilde{M} &= \tau_z\otimes i\sigma_z.
\end{aligned}
$$

Equation (A38) does not have a SPMT with or without $C\tilde{P}$. Thus, the line node remains stable under the map from the P+D class to the D class.

Next, for the case of (d), both the P+DIII class with even parity and the DIII class have the topologically stable line node as shown in Table I. Similarly, we can construct the map from a topologically nontrivial Hamiltonian of the P+DIII class with even parity to that of the DIII class. The Dirac model of this case is given by

$$
\begin{aligned}
H_1 &= k_1\tau_z\otimes 1_{2\times 2} + k_2\tau_y\otimes\sigma_y,\\
C\tilde{P} &= (\tau_x\otimes 1_{2\times 2})K, \qquad \text{(A39)}\\
CT &= \tau_x\otimes i\sigma_y.
\end{aligned}
$$

By Eq. (A39), there is no SPMT, regardless of the existence of $C\tilde{P}$. Thus, the line node remains stable under the map from the P+DIII class to the DIII class.

[1] A. J. Legget, Rev. Mod. Phys. **47**, 331 (1975).
[2] M. Sigrist and K. Ueda, Rev. Mod. Phys. **63**, 239 (1991).
[3] E. I. Blount, Phys. Rev. B **32**, 2935 (1985).
[4] R. Joynt and L. Taillefer, Rev. Mod. Phys. **74**, 235 (2002).
[5] Y. Yanase and M. Ogata, J. Phys. Soc. Jpn. **72**, 673 (2003).
[6] M. Sato, Phys. Rev. B **73**, 214502 (2006).
[7] B. Béri, Phys. Rev. B **81**, 134515 (2010).
[8] G. E. Volovik, *The Universe in a Helium Droplet* (Oxford University Press, New York, 2003).
[9] P. Hořava, Phys. Rev Lett. **95**, 016405 (2005).
[10] Y. X. Zhao and Z. D. Wang, Phys. Rev. Lett. **110**, 240404 (2013).
[11] M. Sato, Y. Tanaka, K. Yada, and T. Yokoyama, Phys. Rev. B **83**, 224511 (2011).
[12] K. Yada, M. Sato, Y. Tanaka, and T. Yokoyama, Phys. Rev. B **83**, 064505 (2011).
[13] Y. Tanaka, M. Sato, and N. Nagaosa, J. Phys. Soc. Jpn. **81**, 011013 (2012).
[14] A. P. Schnyder and S. Ryu, Phys. Rev. B **84**, 060504(R) (2011).
[15] P. M. R. Brydon, A. P. Schnyder, and C. Timm, Phys. Rev. B **84**, 020501(R) (2011).
[16] A. P. Schnyder, P. M. R. Brydon, and C. Timm, Phys. Rev. B **85**, 024522 (2012).
[17] A. P. Schnyder, C. Timm, and P. M. R. Brydon, Phys. Rev. Lett. **111**, 077001 (2013).
[18] S. Matsuura, P.-Y. Chang, A. P. Schnyder, and S. Ryu, New J. Phys. **15**, 065001 (2013).
[19] M. F. Atiyah, R. Bott, and A. Shapiro, Topology **3**, 3 (1964).
[20] M. Karoubi, *K-Theory: An Introduction* (Springer, New York, 1978).
[21] M. Sato, Phys. Rev. B **81**, 220504(R) (2010).
[22] We subtract the constant term from H_{k_0} and choose an appropriate basis, making H_{k_0} an irreducible matrix. Also, when $\dim H_{k_0} = N$, our classification is applicable only in the stable regime $N > p/2$ for the complex case (C_i) and $N > p + 1$ for the real case (R_j).
[23] K. Shiozaki and M. Sato, arXiv:1403.3331.
[24] M. Zirnbauer, J. Math. Phys. **37**, 4986 (1996).
[25] A. Altland and M. R. Zirnbauer, Phys. Rev. B **55**, 1142 (1997).
[26] Y. X. Zhao and Z. D. Wang, Phys. Rev. B **89**, 075111 (2013).
[27] A. Kitaev, AIP Conf. Proc. **1134**, 22 (2009).
[28] M. Stone, C.-K. Chiu, and A. Roy, J. Phys. A: Math. Theor. **44**, 045001 (2011).
[29] G. Abramovici and P. Kalugin, Int. J. Geom. Methods Mod. Phys. **09**, 1250023 (2012).
[30] T. Morimoto and A. Furusaki, Phys. Rev. B **88**, 125129 (2013).
[31] X.-G. Wen, Phys. Rev. B **85**, 085103 (2012).
[32] K. Izawa, Y. Kasahara, Y. Matsuda, K. Behnia, T. Yasuda, R. Settai, and Y. Onuki, Phys. Rev. Lett. **94**, 197002 (2005).
[33] I. Bonalde, W. Bramer-Escamilla, and E. Bauer, Phys. Rev. Lett. **94**, 207002 (2005).
[34] C. R. Hu, Phys. Rev. Lett. **72**, 1526 (1994).
[35] Y. Tanaka and S. Kashiwaya, Phys. Rev. Lett. **74**, 3451 (1995).
[36] S. Kashiwaya and Y. Tanaka, Rep. Prog. Phys. **63**, 1641 (2000).
[37] For the M^+ class, the reflection symmetry satisfies $[\tilde{M},H] = [\tilde{M},C] = 0$ on the reflection plane, namely, H is block diagonalized by an eigenvalue of the reflection symmetry and each sector does not have PHS. The absence of PHS in the sector implies that the stability of the line node is directly determined by that of the Fermi surface intersecting with the reflection plane. In fact, the reflection sector belongs to the topologically nontrivial state of the A class in the AZ classes. Similarly, for the M^{+-} case, the commutation relations are given by $[\tilde{M},H] = [\tilde{M},C] = \{\tilde{M},T\} = 0$. Hence PHS also breaks in the reflection sector, but the TRS remains in each sector, i.e., the reflection sector belongs to the AII class of the AZ classes.
[38] π-SRS is equivalent with $U(1)$-SRS around a quantization axis in the mean-field level. We choose the π-SRS as a sufficient condition of SRS, since π-SRS is a looser condition than $U(1)$-SRS.
[39] For the E_{2u} state of $\mathrm{UPt_3}$ B phase, provided that $\boldsymbol{d} \parallel \boldsymbol{z}$, the line node is protected by the mirror reflection $\tilde{M} = i\tau_0\sigma_z$ and the SRS $\tilde{U}_z = i\tau_z\sigma_z$. This is proved as follows. The combined operator $i\tilde{M}\tilde{U}_z = -i\tau_z\sigma_0$ gives a new reflection operator satisfying $(i\tilde{M}\tilde{U}_z)^2 = -1$ and $[C\tilde{P}, i\tilde{M}\tilde{U}_z] = 0$. Thus $i\tilde{M}\tilde{U}$ belongs to the M^+ class, which has a stable line node.
[40] J. Hara and K. Nagai, Prog. Theor. Phys. **76**, 1237 (1986).
[41] P. Goswami and A. H. Nevidomskyy, arXiv:1403.0924.
[42] T. Löfwander, V. S. Shumeiko, and G. Wendin, Supercond. Sci. Technol. **14**, R53 (2001).
[43] M. Matsumoto and H. Shiba, J. Phys. Soc. Jpn. **64**, 1703 (1995).
[44] H. R. Ott, H. Rudigier, T. M. Rice, K. Ueda, Z. Fisk, and J. L. Smith, Phys. Rev. Lett. **52**, 1915 (1984).
[45] C. Geibel, S. Thies, D. Kaczorowski, A. Mehner, A. Grauel, B. Seidel, U. Ahlheim, R. Helfrich, K. Petersen, C. D. Bredl, and F. Steglich, J. Phys. B: Condens. Matter **83**, 305 (1991).
[46] S. Sasaki, M. Kriener, K. Segawa, K. Yada, Y. Tanaka, M. Sato, and Y. Ando, Phys. Rev. Lett. **107**, 217001 (2011).
[47] T. Micklitz and M. R. Norman, Phys. Rev. B **80**, 100506(R) (2009).
[48] Y. Tsutsumi, M. Ishikawa, T. Kawakami, T. Mizushima, M. Sato, M. Ichioka, and K. Machida, J. Phys. Soc. Jpn. **82**, 113707 (2013).
[49] A. Yamakage, K. Yada, M. Sato, and Y. Tanaka, Phys. Rev. B **85**, 180509(R) (2012).
[50] S. A. Yang, H. Pan, and F. Zhang, arXiv:1402.7070.
[51] A. H. Castro Neto, F. Guinea, N. M. R. Peres, K. S. Novoselov, and A. K. Geim, Rev. Mod. Phys. **81**, 109 (2009).
[52] S. Katayama, A. Kobayashi, and Y. Suzumura, J. Phys. Soc. Jpn. **75**, 054705 (2006); A. Kobayashi and S. Katayama, *ibid.* **76**, 034711 (2007).
[53] S. Ryu, A. P. Schnyder, A. Furusaki, and A. W. W. Ludwig, New J. Phys. **12**, 065010 (2010).
[54] C.-K. Chiu, H. Yao, and S. Ryu, Phys. Rev. B **88**, 075142 (2013).